2006 IEEE International Conference on
Systems, Man, and Cybernetics
October 8-11, 2006, Taipei, Taiwan

Self-Organizing Neural-Network-Based Adaptive Control for Linear Ultrasonic Motor

Chun-Fei Hsu, *Member, IEEE*, and Tsu-Tian Lee, *Fellow, IEEE*

***Abstract*—In this paper, an self-organizing neural-network-based adaptive control (SONNAC) system is developed. The SONNAC system is comprised of a neural controller and a compensation controller. The neural controller utilizes a self-organizing neural network (SONN) to mimic an ideal controller, and the compensation controller is designed to compensate for the approximation error between the neural controller and the ideal controller. When the approximation performance of the SONN is not good enough, the SONN can create new neurons in the hidden layer to decrease the approximation error. Moreover, the adaptive laws of controller parameters are derived in the sense of Lyapunov, so that the stability of the system can be guaranteed. Finally, to investigate the effectiveness of the proposed SONNAC system, the design methodology is applied to control a linear ultrasonic motor.**

I. Introduction

THE computed torque or inverse dynamics technique is a special application of feedback nonlinear systems. These design methods are based on a good understanding of the controlled system dynamics and its environment; however, it is unpractical to precisely model a complex nonlinear system. To tackle this problem, the neural-network-based control techniques have presented the alternative design approaches for the uncertain nonlinear systems [1-5]. The successful key element is the approximation theory, where the parameterized neural network can approximate the unknown system dynamics or the ideal controller after learning. Some of these learning algorithms are based on the backpropagation algorithm. However, these approaches are difficult to guarantee the stability and robustness of closed-loop system. To overcome this difficulty, some of the learning algorithms are based on the Lyapunov stability theorem. The tuning laws of the neural network have been designed to guarantee the system stability in the Lyapunov sense.

Although the control performances are acceptable in [1-5], the learning algorithm only includes the parameter learning, and they have not considered the structure learning of the neural network. If the number of neurons in the hidden layer is chosen too large, the computation loading is heavy so that they are not suitable for practical applications. If the number of neurons in the hidden layer is chosen too small, the learning performance may be not good enough to achieve desired control performance. To tackle this problem, several self-constructing neural networks, consisting of structure and parameter learning phases, have been proposed [6-8]. These two-phase learning algorithms not only decide the structure of neural network but also adjust the parameters of neural network. Recently, some self-constructing neural networks have been applied to solve several control problems. However, some of them can not guarantee the system stability; and some of them require too complex design procedure to achieve satisfactory performance.

Modern mechanical systems, such as machine tools and automatic inspection machines, often require high-speed high-accuracy linear motions. These linear motions are usually realized using the rotary motors with a mechanical transmission, such as reduction gears and lead screw. These transmission mechanisms not only significantly reduce the linear motion speed and dynamic response, but also introduce the backlash and large friction. To tackle this problem, a linear ultrasonic motor (LUSM) is introduced to apply the linear motion without using any mechanical transmission. The LUSM has much merit, such as high precision, fast control dynamics, large driving force, smaller dimension, high holding force, silence and more minimum step size than the class electromagnetic motors, so that it can be used in many different applications [9]. However, the driving principle of the LUSM is based on the ultrasonic vibration force of piezoelectric ceramic elements and mechanical frictional force. Therefore, its mathematical model is complex, and the motor parameters are time-varying because of increasing temperature and changes in motor drive operating conditions. For control system designs, the conventional control technologies are always based on a good understanding of the controlled system; however, the LUSM dynamic model is difficult to obtain. Therefore, it is very difficult to control the LUSM using the conventional control theory. To tackle this problem, some design techniques have been adopted for the LUSM control [10-12]; however, these design procedures are overly complex or may cause large chattering in the control efforts which will wear the bearing mechanism and excite unmodelled dynamics.

The motivation of this paper is to design a self-organizing neural-network-based adaptive control (SONNAC) system for the LUSM. The SONNAC system is comprised of a neural controller and a compensation controller. The neural controller uses a self-organizing neural network (SONN) to approximate an ideal controller. The compensation controller

Manuscript received December 25, 2005. This work was supported in part by the National Science Council of the Republic of China under Grant NSC 93-2213-E-155-038.

Chun-Fei Hsu is with the Department of Electrical and Control Engineering, National Chiao-Tung University, Hsinchu 300, Taiwan, Republic of China (e-mail: fei@cn.nctu.edu.tw).

Tsu-Tian Lee is with the Department of Electrical Engineering, National Taipei University of Technology, Taipei 106, Taiwan, Republic of China (e-mail: ttlee@ntut.edu.tw).

is designed to recover the residual of the approximation error. The learning phase of SONNAC includes a structure learning and a parameter learning. In the structure learning phase, the developed SONN can on-line create new neurons in the hidden layer as the approximation performance is not good enough, thus the learning capability and flexibility can be upgraded. In the parameter learning phase, the controller parameters can be on-line tuned based on the Lyapunov function, so that the stability of the closed-loop system can be guaranteed. Finally, the experiment results are performed to demonstrate the effectiveness of the proposed SONNAC design method for LUSM.

II. MODELING OF LINEAR ULTRASONIC MOTOR

The structure of the LUSM is a large face of a relatively thin rectangular piezoelectric ceramic device. The driving principles of the LUSM are based on the ultrasonic vibration force of piezoelectric ceramic element and mechanical frictional force. Figure 1 shows the principal structure of the LUSM considered in this study [9]. The stator vibrator is fitted with bending and longitudinal piezoelectric actuators. They are driven by two electrical sources of identical frequency, but with a phase difference that is carefully controlled. At the vibration tip, an elliptical motion is thus created, resultant of the elliptical and longitudinal motion. The bending actuators convert a large electrical power to mechanical output and the longitudinal actuator dynamically changes the force along the pre-load direction to adjust the frictional force between the stator and the rotor. Friction is inevitable in the LUSM. It is a highly complicated process to attempt to build an explicit mathematical friction model for the LUSM because friction plays a dual role: it does not simply contribute to the nonlinear dynamics (e.g., dead zone) of the LUSM, but it also serves as the driving force for the moving part. Therefore, the LUSM dynamic equation is very complicated and the parameters of the elements are not easy to know.

For developing the control law, the LUSM can be described as a second-order nonlinear dynamic equation by the Newton's Law as

$$[M+m]\ddot{x} = F(\mathbf{x}) + G(\mathbf{x})u \tag{1}$$

where M is the mass of the moving table; m is the mass of the payload; $\mathbf{x} = [x\ \dot{x}]^T$ represents the position and velocity of the moving table; $F(\mathbf{x})$ is the nonlinear dynamic function including friction, ripple force and external disturbance; $G(\mathbf{x})$ is the gain of the LUSM resonant inverter; and u is the input force to the LUSM. Rewriting (1), the dynamic equation of the LUSM can be obtained as

$$\begin{aligned}\ddot{x} &= \frac{F(\mathbf{x})}{M+m} + \frac{G(\mathbf{x})}{M+m}u \\ &= f(\mathbf{x}) + g(\mathbf{x})u\end{aligned} \tag{2}$$

where $f(\mathbf{x}) = \dfrac{F(\mathbf{x})}{M+m}$ and $g(\mathbf{x}) = \dfrac{G(\mathbf{x})}{M+m}$. Since these nonlinear dynamic functions can not be exactly obtained, the LUSM poses an interesting and challenging dilemma to the control problem.

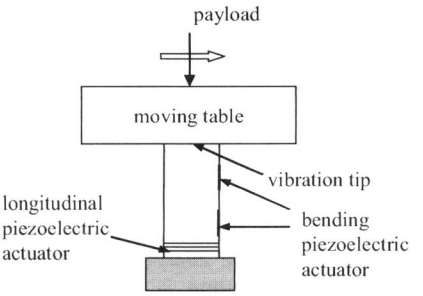

Fig. 1 Structure of the piezoelectric-type linear ultrasonic motor.

III. IDEAL CONTROL

The tracking control problem of the LUSM system is to find a control law so that the state trajectory x can track a reference command x_c. The tracking error is defined as

$$e = x_c - x \tag{3}$$

and a sliding surface is defined as

$$s = \dot{e} + k_1 e + k_2 \int_0^t e(\tau)d\tau \tag{4}$$

where k_1 and k_2 are non-zero positive constants. If the system dynamics are exactly known, an ideal controller can be designed as

$$u^* = u_{eq} + u_{ht} \tag{5}$$

where the equivalent controller u_{eq} is represented as

$$u_{eq} = \frac{1}{g(\mathbf{x})}(-f(\mathbf{x}) + \ddot{x}_c + k_1\dot{e} + k_2 e) \tag{6}$$

and the hitting controller u_{ht} is designed as

$$u_{ht} = \frac{1}{g(\mathbf{x})}\eta\,\mathrm{sgn}(s) \tag{7}$$

where η is a positive constant and sgn(·) is the sign function. Substituting (5), (6) and (7) into (2), yields

$$\dot{s} = -\eta\,\mathrm{sgn}(s). \tag{8}$$

In order to drive the $s \to 0$, consider the Lyapunov function candidate in the following form

$$V_1(s) = \frac{1}{2}s^2. \tag{9}$$

Differentiating (9) with respect to time and using (8), yields

$$\dot{V}_1(s) = s\dot{s} = -\eta|s| \le 0. \tag{10}$$

In summary, the ideal control system presented in (5) can guarantee the system stability in the sense of the Lyapunov. However, if the system dynamics $f(\mathbf{x})$ and $g(\mathbf{x})$ are unknown or perturbed, the ideal control cannot be implemented. Thus, a model-free control technology, which is termed as self-organizing neural-network-based adaptive control (SONNAC), is proposed in the following section to achieve desired tracking performance.

IV. Self-Organizing Neural-Network-Based Adaptive Control

The proposed SONNAC system is comprised of a neural controller and a compensation controller. The neural controller uses a SONN, in which the neurons in the hidden layer can on-line split up as the approximation performance is not good enough, to mimic an ideal controller. The compensation controller is designed to compensate for the approximation error between the neural controller and the ideal controller.

A. Description of Self-Organizing Neural Network

A single-hidden-layer SONN is shown in Fig. 2. The output of this SONN takes the form

$$y = \sum_{i=1}^{m} w_i \, \sigma(v_i s) \tag{11}$$

where s and y are the input and output of the SONN, respectively, σ represents the hidden-layer activation function, v_i is the interconnection weight between the input and hidden layers, and w_j is the interconnection weight between the hidden and output layers. These weights will be on-line adjusted in the following derivation. The activation function in this paper is considered as a sigmoid function

$$\sigma(z) = \frac{1}{(1+e^{-z})}. \tag{12}$$

By collecting all the weights of the SONN, equation (11) can be expressed in a vector form as

$$y = \mathbf{W}^T \sigma(\mathbf{V}s) \tag{13}$$

where $\mathbf{V} = [v_1, v_2, ..., v_m] \in R^m$ and $\mathbf{W} = [w_1, w_2, ..., w_m] \in R^m$. A main property of neural network regarding feedback control purpose is the universal function approximation property. In general, the approximation error decreases as the net size m increases. In general, the number of neurons in hidden layer should be determined by trial-and-error to achieve favorable approximation.

To tackle this problem, this paper proposed a simple disjunction algorithm such that the k-th neuron in the hidden layer splits up at the N-th sampling time, if the following condition is satisfied

$$\frac{|\dot{v}_k| + |\dot{w}_k|}{\sum_{i=1}^{n} (|\dot{v}_i| + |\dot{w}_i|)} \geq \theta, \quad k = 1,2,...,m \tag{14}$$

where θ denotes a disjunction threshold value. When the approximated nonlinear functions are too complex, the disjunction threshold value should be chosen as a small value so that the neurons can be easily created. The tuning laws $\dot{v}_i$ and $\dot{w}_i$ will be derived in the next subsection. The proposed disjunction algorithm is derived from the observation that if the left hand side of (14) is larger than the disjunction threshold value, which implies the precise approximation is hard to capture because the updating of the weight values is relatively large. For that reason, if condition (14) is satisfied, then a new neuron is created to spread the relatively large variation of the weights. As shown in Fig. 3, the k-th neuron satisfying (14) is divided into two neurons, and the newly created neuron is denoted by k'-th neuron. The new weights connected to the k'-th neuron are decided as follows

$$v_{k'}(N+1) = v_k(N) \tag{15}$$

$$w_{k'}(N+1) = \alpha w_k(N) \tag{16}$$

where α is a positive constant. The weights connected to the k-th neuron are determined as follows

$$v_k(N+1) = v_k(N) \tag{17}$$

$$w_k(N+1) = (1-\alpha) w_k(N). \tag{18}$$

This method is induced from the facts that the weights connected to the newly created neuron will share the large variations of the weights.

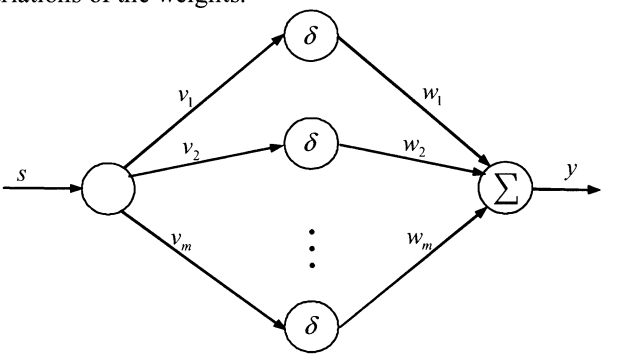

Fig. 2. The structure of self-organizing neural network.

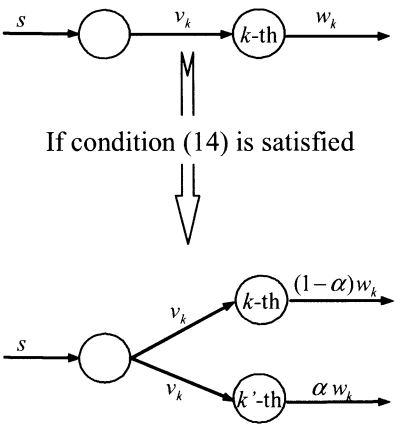

Fig. 3. Schematic illustration of the disjunction algorithm.

B. Design of SONNAC

The developed SONNAC system is shown in Fig. 4; the controller is comprised of a neural controller and a compensation controller

$$u = u_{nn} + u_{cp}. \tag{19}$$

The neural controller u_{nn} is utilized to approximate the ideal controller and the compensation controller u_{cp} is designed to compensate for the approximation error between the neural controller and the ideal controller. Substituting (19) into (1), yields

$$\ddot{x} = f(\mathbf{x}) + g(\mathbf{x})(u_{nn} + u_{cp}). \tag{20}$$

Using (5) and (20), the error dynamic equation is obtained

$$\dot{s} = g(\mathbf{x})(u^* - u_{nn} - u_{cp} - \eta \operatorname{sgn}(s)) . \quad (21)$$

By the universal approximation theorem, an optimal approximator can be designed to approximate the ideal controller, such that

$$u^* = u_{nn}^* + \Delta = \mathbf{W}^{*T}\sigma(\mathbf{V}^* s) + \Delta = \mathbf{W}^{*T}\boldsymbol{\sigma}^* + \Delta \quad (22)$$

where $\mathbf{V}^*$ and $\mathbf{W}^*$ are the optimal vectors of SONN and Δ is the approximation error. Let the number of optimal neurons be n^* and the neurons be divided into two parts. The first part contains n neurons which are the activated part and the secondary part contains $n^* - n$ neurons which do not exist yet. Thus, the optimal weights of NN $\mathbf{V}^*$ and $\mathbf{W}^*$ are classified in two parts such as

$$\mathbf{V}^* = [\mathbf{V}_a^* \quad \mathbf{V}_i^*] \text{ and } \mathbf{W}^* = \begin{bmatrix} \mathbf{W}_a^* \\ \mathbf{W}_i^* \end{bmatrix} \quad (23)$$

where $\mathbf{V}_a^* \in R^n$ and $\mathbf{W}_a^* \in R^n$ are activated parts, and $\mathbf{V}_i^* \in R^{(n^*-n)}$ and $\mathbf{W}_i^* \in R^{(n^*-n)}$ are inactivated parts, respectively. Since the optimal NN weights that are needed to best approximate the ideal controller are unobtainable, an estimation of u_{nn} is given by

$$u_{nn} = \hat{\mathbf{W}}_a^T \sigma(\hat{\mathbf{V}}_a s) = \hat{\mathbf{W}}_a^T \hat{\boldsymbol{\sigma}}_a \quad (24)$$

where $\hat{\mathbf{V}}_a$ and $\hat{\mathbf{W}}_a$ are the estimated values of the optimal weights $\mathbf{V}_a^*$ and $\mathbf{W}_a^*$, respectively. Define the estimated error $\tilde{u}$ as

$$\begin{aligned} \tilde{u} &= u^* - u_{nn} \\ &= \mathbf{W}_a^{*T}\boldsymbol{\sigma}_a^* + \mathbf{W}_i^{*T}\boldsymbol{\sigma}_i^* - \hat{\mathbf{W}}_a^T\hat{\boldsymbol{\sigma}}_a + \Delta \\ &= \tilde{\mathbf{W}}_a^T\hat{\boldsymbol{\sigma}}_a + \hat{\mathbf{W}}_a^T\tilde{\boldsymbol{\sigma}}_a + \tilde{\mathbf{W}}_a^T\tilde{\boldsymbol{\sigma}}_a + \mathbf{W}_i^{*T}\boldsymbol{\sigma}_i^* + \Delta \end{aligned} \quad (25)$$

where $\boldsymbol{\sigma}_a^* = \sigma(\mathbf{V}_a^* \mathbf{x})$, $\boldsymbol{\sigma}_i^* = \sigma(\mathbf{V}_i^* \mathbf{x})$, $\tilde{\boldsymbol{\delta}}_a = \boldsymbol{\delta}_a^* - \hat{\boldsymbol{\delta}}_a$, $\tilde{\mathbf{W}}_a = \mathbf{W}_a^* - \hat{\mathbf{W}}_a$ and $\tilde{\mathbf{V}}_a = \mathbf{V}_a^* - \hat{\mathbf{V}}_a$. The Taylor series expansion of $\boldsymbol{\sigma}_a^*$ with respect to $\hat{\mathbf{V}}_a s$ can be derived as

$$\boldsymbol{\sigma}_a^* = \hat{\boldsymbol{\sigma}}_a + \boldsymbol{\sigma}_a' \tilde{\mathbf{V}}_a s + \mathbf{h} \quad (26)$$

where $\boldsymbol{\sigma}_a'$ is the Jacobian and $\mathbf{h}$ is a vector of higher-order terms. Therefore,

$$\tilde{\boldsymbol{\sigma}}_a = \boldsymbol{\sigma}_a' \tilde{\mathbf{V}}_a^T s + \mathbf{h} . \quad (27)$$

Substituting (27) into (25), yields

$$\tilde{u} = \tilde{\mathbf{W}}_a^T \hat{\boldsymbol{\sigma}}_a + \hat{\mathbf{W}}_a^T \boldsymbol{\sigma}_a' \tilde{\mathbf{V}}_a s + \varepsilon \quad (28)$$

where $\varepsilon = \tilde{\mathbf{W}}_a^T \tilde{\boldsymbol{\sigma}}_a + \mathbf{W}_i^{*T} \boldsymbol{\sigma}_i^* + \tilde{\mathbf{W}}_a^T \mathbf{h} + \Delta$ is assumed to be bounded by $|\varepsilon| \le E$ where E is a positive constant. However, the bound of approximation error E is difficult to measure in practical applications. Thus, using the approximation error equation (28), equation (29) can be rewritten as

$$\dot{s}(t) = g(\mathbf{x})(\tilde{\mathbf{W}}_a^T \hat{\boldsymbol{\sigma}}_a + s\tilde{\mathbf{V}}_a^T \boldsymbol{\sigma}_a'^T \hat{\mathbf{W}}_a + \varepsilon - u_{cp} - \eta \operatorname{sgn}(s)) . \quad (29)$$

In this derivation, $\hat{\mathbf{W}}_a^T \boldsymbol{\sigma}_a' \tilde{\mathbf{V}}_a s = [\hat{\mathbf{W}}_a^T \boldsymbol{\sigma}_a' \tilde{\mathbf{V}}_a s]^T$ is used since it is a scale. Therefore, the following theorem can be stated and proved.

Theorem 1: Consider a linear ultrasonic motor system expressed by (1). If the self-organizing neural-network-based adaptive control system is designed as (19). A self-organizing neural network splits up the neurons in the hidden layer if condition (14) is satisfied. The adaptation laws of activated parts $\hat{\mathbf{V}}_a$ and $\hat{\mathbf{W}}_a$ are designed as

$$\dot{\hat{\mathbf{V}}}_a = -\dot{\tilde{\mathbf{V}}}_a = \eta_V s^2 g(\mathbf{x}) \boldsymbol{\sigma}_a'^T \hat{\mathbf{W}}_a \quad (30)$$

$$\dot{\hat{\mathbf{W}}}_a = -\dot{\tilde{\mathbf{W}}}_a = \eta_W s\, g(\mathbf{x}) \hat{\boldsymbol{\sigma}}_a \quad (31)$$

where η_V and η_W are the positive learning-rates. The compensation controller is designed as

$$u_{cp} = \hat{E} \operatorname{sgn}(s) \quad (32)$$

where $\hat{E}$ is the estimation of the approximation error bound with the estimation law given as

$$\dot{\hat{E}} = -\dot{\tilde{E}} = \eta_E |s\, g(\mathbf{x})| \quad (33)$$

where η_E is a positive learning-rate. Then, the stability of the adaptive self-structuring neural network control system can be guaranteed.

Proof:

Define a Lyapunov function candidate in the following form

$$V_2(s, \tilde{\mathbf{V}}_a, \tilde{\mathbf{W}}_a, \tilde{E}) = \frac{1}{2}s^2 + \frac{1}{2\eta_V}\tilde{\mathbf{V}}_a^T\tilde{\mathbf{V}}_a + \frac{1}{2\eta_W}\tilde{\mathbf{W}}_a^T\tilde{\mathbf{W}}_a + \frac{1}{2\eta_E}\tilde{E}^2 . \quad (34)$$

where $\tilde{E} = E - \hat{E}$. Differentiating (34) with respect to time and using (29), and (30)-(33), gives

$$\begin{aligned} \dot{V}_2(s, \tilde{\mathbf{V}}_a, \tilde{\mathbf{W}}_a, \tilde{E}) &= s\dot{s} + \frac{\tilde{\mathbf{V}}_a^T \dot{\tilde{\mathbf{V}}}_a}{\eta_V} + \frac{\tilde{\mathbf{W}}_a^T \dot{\tilde{\mathbf{W}}}_a}{\eta_W} + \frac{\tilde{E}\dot{\tilde{E}}}{\eta_E} \\ &= -\eta\, g(\mathbf{x})|s| + \varepsilon s\, g(\mathbf{x}) - E|s\, g(\mathbf{x})| \\ &\le -(E - |\varepsilon|)|s\, g(\mathbf{x})| \le 0 . \end{aligned} \quad (35)$$

If the system dynamic $g(\mathbf{x})$ is unavailable, the $g(\mathbf{x})$ in the adaptive algorithms can be reorganized as $|g(\mathbf{x})|\operatorname{sgn}(g(\mathbf{x}))$ in practical applications. Therefore, the learning algorithms for the SONNAC shown in (30), (31) and (33) can be reconstructed as follows:

$$\dot{\hat{\mathbf{V}}}_a = \eta_1 s^2 s \boldsymbol{\sigma}_a'^T \hat{\mathbf{W}}_a \quad (36)$$

$$\dot{\hat{\mathbf{W}}}_a = \eta_2 s \hat{\boldsymbol{\sigma}}_a \quad (37)$$

$$\dot{\hat{E}} = -\dot{\tilde{E}} = \eta_3 |s| \quad (38)$$

in which $\eta_1 = \eta_V |g(\mathbf{x})|$, $\eta_2 = \eta_W |g(\mathbf{x})|$ and $\eta_3 = \eta_E |g(\mathbf{x})|$. The η_1 , η_2 and η_3 can be taken as new learning-rates.

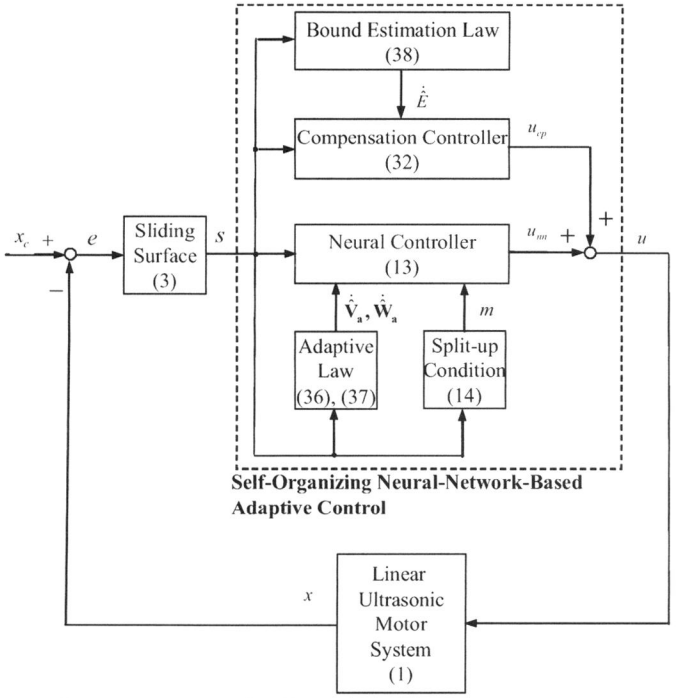

Fig. 4. SONNAC for linear ultrasonic motor system.

V. Experimental Results

The computer control experimental system for the LUSM is shown in Fig. 5. A servo control card is installed in the control computer, which included multi-channels of D/A, A/D, PIO and encoder interface circuits. The position of the moving table is feedback using a linear scale. The proposed SONNAC system is realized in the Pentium using the "Turbo C" language. The control interval of the control system are set as 2 ms. The control objective is to control the moving table to follows a 0.035m periodic step command. Moreover, a second-order transfer function $\frac{64}{s^2+16s+64}$ is chosen as the reference model for the step command.

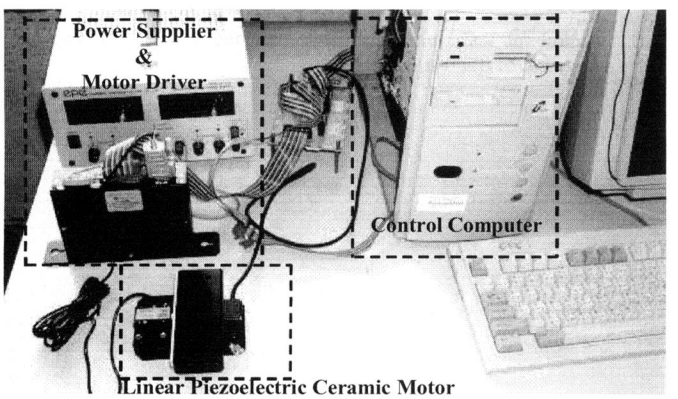

Fig. 5 Computer-controlled linear ultrasonic motor system.

To illustrate the effectiveness of the proposed design method, a comparison between a fixed-structured neural network control in [5] and the proposed SONNAC is made. The experimental results of fixed-structured neural network control are shown in Fig. 6. The tracking responses are shown in Figs. 6(a) and 6(c); and the torque input are shown in Figs. 6(b) and 6(d) for 7 and 20 hidden neurons, respectively. Experimental results show that the robust tracking performance has been achieved for different hidden neurons. If the number of hidden neurons is chosen too small, the convergence of the tracking error is slow. On the other hand, if the number of hidden neurons is chosen too large, the computation loading is heavy.

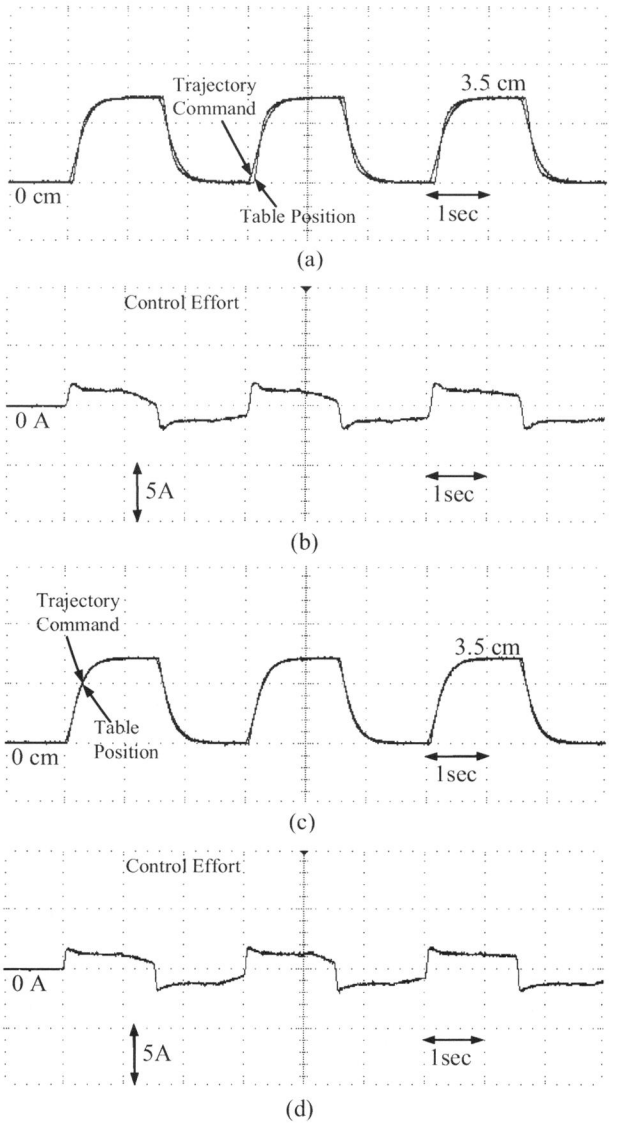

Fig. 6 Experimental results of fixed-structured neural network control.

Then, the developed SONNAC is applied to control the LUSM. The parameters in the proposed SONNC system are selected as $k_1 = 2$, $k_2 = 1$, $\eta_1 = 50$, $\eta_2 = 50$, $\eta_3 = 0.1$, $\alpha = 0.3$, and $\theta = 0.5$. The experimental results of SONNAC are shown in Fig. 7. The tracking response is shown in Figs. 7(a); the torque input is shown in Figs. 7(b), and the number of the hidden node is shown in Fig. 7(c). It shows that the

favorable tracking performance can be achieved for the proposed SONNAC after the structure and parameter learning phases. Moreover, the SONNAC can on-line create new neurons in the hidden layer as the approximation of neural network is not good enough.

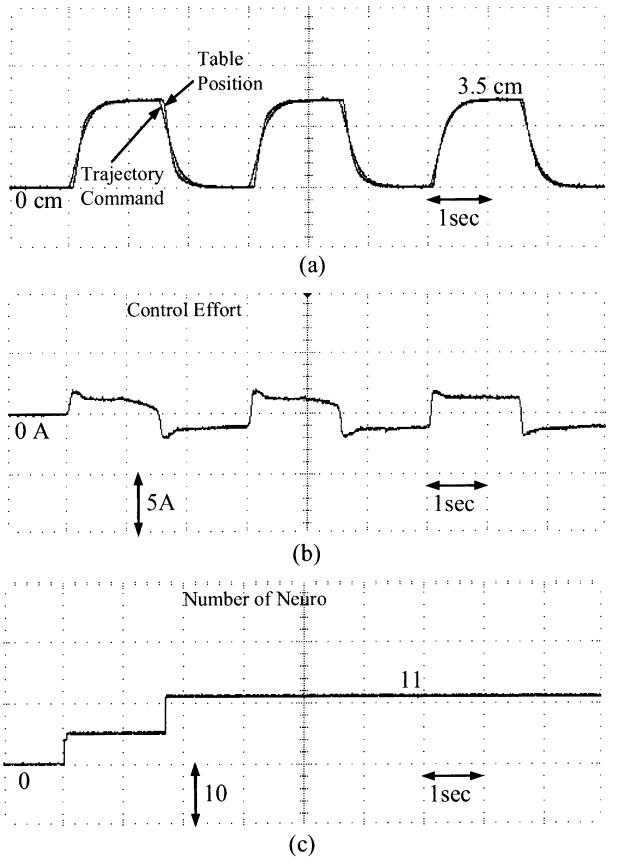

Fig. 7 Experimental results of SONNAC.

VI. Conclusions

This paper developed a self-organizing neural-network-based adaptive control (SONNAC) system, which is comprised of a neural controller and a compensation controller. In the neural controller design, a self-organizing neural network is utilized to mimic an ideal controller. In the compensation controller design, an error estimation mechanism is investigated to estimate the bound of approximation error. The major contributions of this paper are: 1) the successful development of an SONNAC, in which the Lyapunov stability theorem is used to derive the on-line learning algorithms. 2) the self-structuring neural network has been created with easy split-up algorithm of hidden neurons to achieve favorable learning performance. 3) the successful application of the SONNAC to control a linear ultrasonic motor.

Acknowledgment

The authors appreciate the partial financial support from National Science Council of the Republic of China under Grant NSC 93-2213-E-155-038.

References

[1] F. L. Lewis, A. Yesildirek, and K. Liu, "Multilayer neural-net robot controller with guaranteed tracking performance," *IEEE Trans. Neural Netw.*, 7 (1996) 388-399.

[2] Y. G. Leu, W. Y. Wang, and T. T. Lee, "Robust adaptive fuzzy-neural controllers for uncertain nonlinear systems," *IEEE Trans. Robotics and Automation,* 15 (1999) 805-817.

[3] F. J. Lin and R. J. Wai, "Hybrid computed torque controlled motor-toggle servomechanism using fuzzy neural network uncertainty observer," *Neurocomputing* 48 (2002) 403-422.

[4] J. Q. Huang and F. L. Lewis, "Neural-network predictive control for nonlinear dynamic systems with time-delay," *IEEE Trans. Neural Netw.*, 14 (2003) 377-389.

[5] C. M. Lin and C. F. Hsu, "Neural network hybrid control for antilock braking systems," *IEEE Trans. Neural Netw.*, 14 (2003) 351-359.

[6] C. T. Lin, "A neural fuzzy control system with structure and parameter learning," *Fuzzy Sets Syst.*, 70 (1995) 183-212.

[7] C. F. Juang and C. T. Lin, "An online self-constructing neural fuzzy inference network and its applications," *IEEE Trans. Fuzzy Systems*, 6 (1998) 12-32.

[8] F. J. Lin, C. H. Lin, and P. H. Shen, "Self-constructing fuzzy neural network speed controller for permanent-magnet synchronous motor drive," *IEEE Trans. Fuzzy Systems*, 9 (2001) 751-759.

[9] T. Sashida and T. Kenjo, *An Introduction to Ultrasonic Motors*, Clarendon Press, Oxford, 1993.

[10] K. K. Tan, T. H. Lee and H. X. Zhou, "Micro-positioning of linear-piezoelectric motors based on a learning nonlinear PID controller," *IEEE / ASME Trans. Mechatoronics*, 6, (2001), 428-436.

[11] R. J. Wai, F. J. Lin, R. Y. Duan, K. Y. Hsieh and J. D. Lee, "Robust fuzzy neural network control for linear ceramic motor via backstepping design technique," *IEEE Trans. Fuzzy Syst.*, 10, (2002), 102-112.

[12] Y. F. Peng, R. J. Wai and C. M. Lin, "Implementation of LLCC-resonant driving circuit and adaptive CMAC neural network control for linear piezoelectric ceramic motor," *IEEE Trans. Ind. Electron.* 51, (2004), 35-48.